Mathematical Biosciences and Engineering

http://www.aimspress.com/journal/mbe

MBE, 19(8): 8035–8056.
DOI: 10.3934/mbe.2022376
Received: 05 March 2022
Revised: 01 April 2022
Accepted: 23 May 2022
Published: 01 June 2022

Research article

Mathematical modeling of mutated COVID-19 transmission with quarantine, isolation and vaccination

Fang Wang, Lianying Cao*and Xiaoji Song

Department of Mathematics, Northeast Forestry University, Harbin 150040, China

* **Correspondence:** Email: lycao200153@sina.com.

Abstract: Multiple variants of SARS-CoV-2 have emerged but the effectiveness of existing COVID-19 vaccines against variants has been reduced, which bring new challenges to the control and mitigation of the COVID-19 pandemic. In this paper, a mathematical model for mutated COVID-19 with quarantine, isolation and vaccination is developed for studying current pandemic transmission. The basic reproduction number $\mathscr{R}_0$ is obtained. It is proved that the disease free equilibrium is globally asymptotically stable if $\mathscr{R}_0 < 1$ and unstable if $\mathscr{R}_0 > 1$. And numerical simulations are carried out to illustrate our main results. The COVID-19 pandemic mainly caused by Delta variant in South Korea is analyzed by using this model and the unknown parameters are estimated by fitting to real data. The epidemic situation is predicted, and the prediction result is basically consistent with the actual data. Finally, we investigate several critical model parameters to access the impact of quarantine and vaccination on the control of COVID-19, including quarantine rate, quarantine effectiveness, vaccination rate, vaccine efficacy and rate of immunity loss.

Keywords: COVID-19; quarantine; isolation; vaccination; variants

1. Introduction

Corona Virus Disease 2019 (COVID-19), caused by SARS-CoV-2, has been seriously impacting the world since the end of 2019 [1]. As of April 13, 2022, there have been over 499 million confirmed cases of COVID-19, including over 6 million deaths all over the world [2].

Since the outbreak of COVID-19, many scholars have used different methods to study its transmission [3], such as neural network [4], time series analysis [5] and kinetic modeling [6].

Dynamics models have played a key role in studying the development of things and assessing the impact of different intervention strategies [7, 8]. In particular, during the COVID-19 outbreak, multiple dynamics models have been developed to investigate its spread and control.

Before the availability of effective vaccines, non-pharmaceutical interventions strategies (NPIs)

were taken into account controlling the pandemic transmission, such as lockdowns, the use of face-masks in public, quarantine of close contacts, isolation of confirmed cases, among others [9]. Ngonghala et al. [10] proposed a detailed mathematical model of COVID-19 that combined quarantine and isolation to assess the impact of NPIs on combating and mitigating the burden of COVID-19. Their results indicated that the early implementation (and enhancement of effectiveness) of these intervention measures is obviously critically-important to curtail COVID-19 transmission. NPIs could mitigate the spread of the virus, but it is not the permanent solution to the problem [11].

Since January 2021, more than ten types of vaccines against SARS-CoV-2 have been fully or limitedly approved and used clinically [12]. And many countries are starting vaccination campaigns, which has improved the global epidemic to some extent [13]. Iboi et al. [14] developed a mathematical model for assessing the impact of an anti-COVID-19 vaccine on the spread of COVID-19 in the United States. This study showed that the prospect of eliminating COVID-19 in the US using the imperfect hypothetical vaccine is promising. Moreover, the integration of vaccination and physical distancing interventions, can result in better pandemic prevention [15]. Zou et al. [16] established a multiple patch coupled model to explore the impact of vaccination and NPIs on the control of COVID-19 and the results indicated that effective vaccination has positive impact on prevention of pandemic transmission and the joint implementation of vaccination and quarantine ensures the controllability of the epidemic.

However, new variants of COVID-19 with high transmission rates are spreading around the world and vaccines are less effective in preventing infection than they were for earlier virus variants, which have brought new challenges to the elimination of pandemic [17, 18]. Recently, Li et al. [19] developed a mathematical model of COVID-19 transmission with imperfect vaccination to explore effective and reasonable plans to prevent the spread of Delta variant. Their results found that the optimal control measure is to dynamically adjust three control measures, namely, vaccination, isolation and nucleic acid testing, to achieve the lowest number of infections at the lowest cost. Truszkowska et al. [20] developed an extremely detailed mathematical model, to study the combined effect of booster shot administration and testing practices in this stage of the pandemic.

Motivated by the implement of NPIs, the promotion of vaccination strategy and the emerging of variants of COVID-19, we consider a mathematical model for mutated COVID-19 with quarantine, isolation and vaccination, make some theoretical analysis of the model, verify the applicability of the model by the COVID-19 pandemic mainly caused by Delta variant in South Korea, and finally, assess the impact of quarantine and vaccination on eliminating mutated COVID-19 transmission.

The organization of this paper is as follows. In Section 2, the basic model formulation is discussed. In Section 3 we derive the disease free equilibrium and basic reproduction number $\mathscr{R}_0$. The local asymptotic stability and global asymptotic stability of the model at the disease free equilibrium are proved. In Section 4, the numerical simulation is carried out to verify the correctness of the proof. In Section 5, according to the epidemic data of COVID-19 in South Korea from August 22 to October 20, 2021, unknown parameters are obtained by two-stage fitting, and then the epidemic is predicted, which is compared with the real data to verify the applicability of the model. In Section 6, the impact of quarantine and vaccination on the control of COVID-19 are assessed by numerical simulation. Finally, in Section 7, we give some discussions.

2. Model formulation

We develop an epidemic model, which incorporates the main interventions being implemented to curtail COVID-19 transmission (such as quarantine, isolation and vaccination). We stratify the population as susceptible (S_u), vaccinated (V_u), exposed (E_u), asymptomatically-infectious (I_a), symptomatically-infectious (I_u) and recovered (R) compartments, and further stratify the population to include quarantined susceptible (S_q), quarantined vaccinated (V_q), quarantined exposed (E_q) and hospitalized (I_h) compartments, so that the total population of the model $N(t)$ is divided into 10 compartments, namely

$$N(t) = S_u(t) + S_q(t) + V_u(t) + V_q(t) + E_u(t) + E_q(t) + I_u(t) + I_h(t) + I_a(t) + R(t).$$

For developing the mathematical model, the basic assumptions are as follows:

(i) The recruitment rate (either by birth or by immigration) of the population is given by a constant rate Λ and they are all susceptible.

(ii) Susceptible individuals move to exposed compartment by effective contacts with exposed, symptomatically-infectious or asymptomatically-infectious individuals and after latency period, they become infectious and move to infectious compartment.

(iii) After recovery the individuals have immunity to COVID-19 in a short time.

(iv) A part of vaccinated individuals will lose their immunity and rejoin the susceptible compartment.

(v) After the immunity period, the vaccinated individuals become susceptible again.

(vi) Hospitalization is completely effective.

(vii) The exposed individuals and the asymptomatically-infectious individuals are also infectious, but the infectivity is weaker than that of symptomatically-infectious individuals, measuring by coefficients η_u and η_a respectively($0 < \eta_u, \eta_a < 1$).

(viii) The contact rate c is the same for the individuals in symptomatically-infectious I_u, non-quarantined exposed E_u and the asymptomatically-infectious I_a compartments.

(ix) The latency period is defined as the days from exposure to the onset of illness.

(x) The asymptomatically-infectious compartment I_a includes those with mild symptoms or no clinical symptoms of the COVID-19 at the end of the latency period.

(xi) Considering that the number of people that an infected person can contact per unit time is finite, a more realistic standard incidence is used in the model.

(xii) The vaccinated individuals will not lose immunity during the quarantine period.

(xiii) If the quarantine individuals have symptoms, they will be sent to the hospital.

The assumptions above lead to the flow diagram of the model depicted in Figure 1.

It is worth noting that hospitalization indicates isolation at the hospital in this study. With contact tracing, a proportion, q, of individuals exposed to the virus is quarantined. The quarantined individuals, if infected, move to the compartment E_q and and the remaining individuals can either stay in compartment V_q or S_q, depending on whether they are vaccinated or not. For those individuals who are missed from contact tracing, the situation is similar.

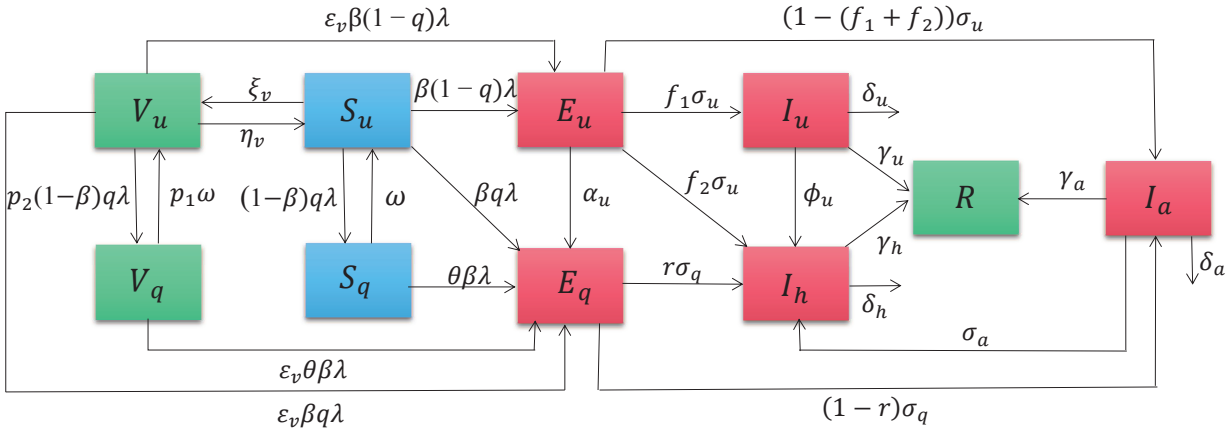

Figure 1. Flow diagram of the model.

The model is given by the following deterministic system of nonlinear differential equations.

$$\begin{aligned}
\frac{dS_u}{dt} &= \Lambda - [\beta(1-q)\lambda + \beta q\lambda + (1-\beta)q\lambda + \xi_v + d]\,S_u + \omega S_q + \eta_v V_u,\\
\frac{dS_q}{dt} &= -(\omega + \theta\beta\lambda + d)S_q + (1-\beta)q\lambda S_u,\\
\frac{dV_u}{dt} &= -[\eta_v + \varepsilon_v\beta(1-q)\lambda + \varepsilon_v\beta q\lambda + p_2(1-\beta)q\lambda + d]\,V_u + \xi_v S_u + p_1\omega V_q,\\
\frac{dV_q}{dt} &= -(p_1\omega + \varepsilon_v\theta\beta\lambda + d)V_q + p_2(1-\beta)q\lambda V_u,\\
\frac{dE_u}{dt} &= -[\alpha_u + f_1\sigma_u + f_2\sigma_u + (1-f_1-f_2)\sigma_u + d]\,E_u + \beta(1-q)\lambda S_u + \varepsilon_v\beta(1-q)\lambda V_u,\\
\frac{dE_q}{dt} &= -\left[r\sigma_q + (1-r)\sigma_q + d\right]E_q + \beta q\lambda S_u + \theta\beta\lambda S_q + \varepsilon_v\beta q\lambda V_u + \varepsilon_v\theta\beta\lambda V_q + \alpha_u E_u,\\
\frac{dI_u}{dt} &= -(\phi_u + \delta_u + \gamma_u + d)I_u + f_1\sigma_u E_u,\\
\frac{dI_h}{dt} &= -(\delta_h + \gamma_h + d)I_h + f_2\sigma_u E_u + r\sigma_q E_q + \phi_u I_u + \sigma_a I_a,\\
\frac{dI_a}{dt} &= -(\sigma_a + \delta_a + \gamma_a + d)I_a + (1-f_1-f_2)\sigma_u E_u + (1-r)\sigma_q E_q,\\
\frac{dR}{dt} &= \gamma_u I_u + \gamma_h I_h + \gamma_a I_a - dR.
\end{aligned} \tag{2.1}$$

where $\lambda(t) = \dfrac{c(I_u + \eta_u E_u + \theta\eta_u E_q + \eta_a I_a)}{S_u + V_u + E_u + I_u + I_a + R + \theta(S_q + E_q + V_q)}$.

The initial conditions for system (2.1) are as follows:

$$\begin{aligned}
&S_u(0) = S_{u0} \geq 0, S_q(0) = S_{q0} \geq 0, V_u(0) = V_{u0} \geq 0, V_q(0) = V_{q0} \geq 0, E_u(0) = E_{u0} \geq 0,\\
&E_q(0) = E_{q0} \geq 0, I_u(0) = I_{u0} \geq 0, I_h(0) = I_{h0} \geq 0, I_a(0) = I_{a0} \geq 0, R(0) = R_0 \geq 0.
\end{aligned} \tag{2.2}$$

The state variables and parameters of the model are described in Tables 1 and 2, respectively.
Let $H(t) = (S_u(t), S_q(t), V_u(t), V_q(t), E_u(t), E_q(t), I_u(t), I_h(t), I_a(t), R(t))$.

Table 1. Description of state variables of the model (2.1).

State variable	Description
S_u	Population of non-quarantined susceptible individuals
S_q	Population of quarantined susceptible individuals
V_u	Population of non-quarantined vaccinated individuals
V_q	Population of quarantined vaccinated individuals
E_u	Population of non-quarantined exposed individuals
E_q	Population of quarantined exposed individuals
I_u	Population of non-hospitalized symptomatically-infectious individuals
I_h	Population of hospitalized symptomatically-infectious individuals
I_a	Population of asymptomatically-infectious individuals with mild or no clinical symptoms of the disease
R	Population of recovered individuals

Lemma 1. *Consider the initial data* $H_i(0) \geq 0, i = 1, 2, ..., 10$. *Then, for any* $t > 0$, *we have the non-negative solution for the system* (2.1).

Proof. Consider $t_1 = sup\{t > 0 : H_i(t) > 0, i = 1, 2, ..., 10\}$. So, $t_1 > 0$. The following result is given using the first equation of the model (2.1),

$$\begin{aligned}\frac{\mathrm{d}S_u}{\mathrm{d}t} &= \Lambda + \omega S_q + \eta_v V_u - (d + \xi_v)S_u - [\beta\lambda + (1-\beta)q\lambda]\, S_u \\ &\geq \Lambda - (d + \xi_v)S_u - [\beta\lambda + (1-\beta)q\lambda]\, S_u.\end{aligned}$$

Then, it can be written as,

$$\frac{\mathrm{d}}{\mathrm{d}t}\left\{S_u(t)exp\left[(d+\xi_v)t + \int_0^t [\beta\lambda(\rho) + (1-\beta)q\lambda(\rho)]d\rho\right]\right\} \geq \Lambda exp\left[(d+\xi_v)t + \int_0^t [\beta\lambda(\rho) + (1-\beta)q\lambda(\rho)]d\rho\right].$$

Thus,

$$\begin{aligned}&S_u(t_1)exp\left[(d+\xi_v)t_1 + \int_0^{t_1} [\beta\lambda(\rho) + (1-\beta)q\lambda(\rho)]\, d\rho\right] - S_u(0) \\ \geq &\int_0^{t_1} \Lambda exp\left[(d+\xi_v)x + \int_0^x [\beta\lambda(\zeta) + (1-\beta)q\lambda(\zeta)]\, d\zeta\right] dx,\end{aligned}$$

so that

$$\begin{aligned}S_u(t_1) \geq &\left(S_u(0) + \int_0^{t_1} \Lambda exp\left[(d+\xi_v)x + \int_0^x [\beta\lambda(\zeta) + (1-\beta)q\lambda(\zeta)]\, d\zeta\right] dx\right) \\ &\times exp\left[-(d+\xi_v)t_1 - \int_0^{t_1} [\beta\lambda(\rho) + (1-\beta)q\lambda(\rho)]\, d\rho\right] > 0.\end{aligned}$$

For the remaining equations, we take the same steps to show $H_i(t) > 0$ $(i = 2, 3, ..., 10)$ for every $t > 0$. □

Table 2. Description of the parameters of the model (2.1).

Parameter	Description	Values
c	Effective contact rate	0.1
β	Probability of infection per contact	0.5
q	Proportion of infectious individuals quarantined at time of exposure	0.05
ξ_v	Vaccination rate (the reciprocal of the time during which everyone has completed vaccination)	0.8
η_v	Rate of immunity loss after vaccination ($1/\eta_v$ is the mean duration of vaccine immunity)	0.56
ε_v	Ineffectiveness of vaccine against COVID-19 variants	0.14
η_u	Modification parameter accounting for the relative infectiousness of individuals in the E_u compartment in relation to individuals in the I_u compartment ($0 < \eta_u < 1$)	0.1
η_a	Modification parameter accounting for the relative infectiousness of individuals in the I_a compartment in relation to individuals in the I_u compartment ($0 < \eta_a < 1$)	0.1
θ	Ineffectiveness of quarantine	0.5
ω	Rate at which individuals in the S_q compartment revert to the S_u compartment ($1/\omega$ is the duration of quarantine)	0.5
α_u	Rate at which individuals in the E_u compartment are detected and placed in quarantine	0.116
$\frac{1}{\sigma_u}(\frac{1}{\sigma_q})$	Latency period for non-quarantined (quarantined) exposed individuals	5.1
σ_a	Rate at which individuals in the I_a compartment are detected and hospitalized	0.309
f_1	Proportion of individuals in the E_u compartment who progress to the I_u compartment at the end of the incubation period ($f_1 + f_2 < 1$)	0.4
f_2	Proportion of individuals in the E_u compartment who progress to the I_h compartment at the end of the incubation period ($f_1 + f_2 < 1$)	0.2
$1 - f_1 - f_2$	Proportion of individuals in the E_u compartment who progress to the I_a compartment	0.4
$r\,(1 - r)$	Proportion of individuals in the E_q compartment who move to the I_h (I_a) compartment	0.7
ϕ_u	Hospitalization rate of individuals in the I_u compartment	0.2
p_1	Modification parameter accounting for the relative release rate of individuals in the V_u compartment in relation to individuals in the S_u compartment	0.5
p_2	Modification parameter accounting for the relative quarantine rate of individuals in the V_u compartment in relation to individuals in the S_u compartment	1
γ_u	Recovery rate for individuals in the I_u compartment	0.1
γ_h	Recovery rate for individuals in the I_h compartment	0.125
γ_a	Recovery rate for individuals in the I_a compartment	0.13978
δ_u	Disease-induced mortality rate for individuals in the I_u compartment	0.015
δ_h	Disease-induced mortality rate for individuals in the I_h compartment	0.015
δ_a	Disease-induced mortality rate for individuals in the I_a compartment	0.075
Λ	Recruitment rate	20
d	Natural death rate	0.2

Let the closed and biologically feasible region be Ω, shown by $\Omega = \left\{(S_u, S_q, V_u, V_q, E_u, E_q, I_u, I_h, I_a, R) \in R_+^{10}, 0 \le S_u, S_q, V_u, V_q, E_u, E_q, I_u, I_h, I_a, R, N \le \frac{\Lambda}{d}\right\}$.

Next, we present the following results for this feasible region.

Lemma 2. *The region Ω is a positively invariant and attracting region for system* (2.1) *with the non-negative initial conditions* (2.2).

Proof. Summing up the ten equations in system (2.1) and considering that all parameters of the model are non-negative, we get

$$\frac{\mathrm{d}N(t)}{\mathrm{d}t} = \Lambda - dN - \delta_a I_a - \delta_u I_u - \delta_h I_h \le \Lambda - dN.$$

Now integrating both sides of the above inequality and using the comparison theorem [21], we obtain

$$0 < N(t) \le \frac{\Lambda}{d} + (N(0) - \frac{\Lambda}{d})e^{-dt}.$$

Clearly, $0 < N(t) \le \frac{\Lambda}{d}$, as $t \to \infty$. If $N(0) \le \frac{\Lambda}{d}$, then $N(t) \le \frac{\Lambda}{d}$. Thus, the region Ω is positive invariant and attracts all the possible solutions of the model (2.1). We will consider the dynamic behavior of model (2.1) on Ω. □

3. Theoretical analysis

3.1. basic reproduction number $\mathscr{R}_0$

Obviously, the model (2.1) always has a disease free equilibrium (DFE) $P_0(S_0, 0, V_0, 0, 0, 0, 0, 0, 0, 0)$, where

$$S_0 = \frac{\Lambda(\eta_v + d)}{d(\eta_v + d + \xi_v)}, V_0 = \frac{\Lambda\xi_v}{d(\eta_v + d + \xi_v)}.$$

The basic reproduction number $\mathscr{R}_0$ will be calculated using the next generation matrix method [22, 23]. It follows that the next generation operator matrices, F and V for the new infection terms and the transition terms, are given, respectively,

$$F = \begin{pmatrix} \eta_u M_1 & \theta\eta_u M_1 & M_1 & 0 & \eta_a M_1 \\ \eta_u M_2 & \theta\eta_u M_2 & M_2 & 0 & \eta_a M_2 \\ 0 & 0 & 0 & 0 & 0 \\ 0 & 0 & 0 & 0 & 0 \\ 0 & 0 & 0 & 0 & 0 \end{pmatrix}, \text{ and } V = \begin{pmatrix} K_1 & 0 & 0 & 0 & 0 \\ -\alpha_u & K_2 & 0 & 0 & 0 \\ -f_1\sigma_u & 0 & K_3 & 0 & 0 \\ -f_2\sigma_u & -r\sigma_q & -\phi_u & K_4 & 0 \\ -(1-f_1-f_2)\sigma_u & -(1-r)\sigma_q & 0 & 0 & K_5 \end{pmatrix},$$

where, $M_1 = c\beta(1-q)\frac{S_0 + \varepsilon_v V_0}{\Lambda/d}$, $M_2 = c\beta q\frac{S_0 + \varepsilon_v V_0}{\Lambda/d}$, $K_1 = \sigma_u + \alpha_u + d$, $K_2 = \sigma_q + d$, $K_3 = \phi_u + \gamma_u + \delta_u + d$, $K_4 = \gamma_h + \delta_h + d$, $K_5 = \sigma_a + \gamma_a + \delta_a + d$. By the definition of the basic reproduction number $\mathscr{R}_0$, we get

$$\mathscr{R}_0 = \rho(FV^{-1}) = \mathscr{R}_{E_u} + \mathscr{R}_{E_q} + \mathscr{R}_{I_u} + \mathscr{R}_{I_a}, \tag{3.1}$$

where,

$$\mathscr{R}_{E_u} = \frac{\eta_u}{K_1} M_1, \qquad \mathscr{R}_{E_q} = \theta\eta_u \left(\frac{\alpha_u}{K_1 K_2} M_1 + \frac{1}{K_2} M_2 \right),$$
$$\mathscr{R}_{I_u} = \frac{f_1 \sigma_u}{K_1 K_3} M_1, \qquad \mathscr{R}_{I_a} = \eta_a \left[\left(\frac{(1 - f_1 - f_2)\sigma_u}{K_1 K_5} + \frac{\alpha_u (1 - r)\sigma_q}{K_1 K_2 K_5} \right) M_1 + \frac{(1 - r)\sigma_q}{K_2 K_5} M_2 \right].$$

The quantity $\mathscr{R}_0$ is the basic reproduction number of the model (2.1). It measures the average number of the new COVID-19 infections generated by a typical infective individual introduced into a population where basic public health interventions (quarantine, isolation, vaccination, etc.) are implemented.

3.2. Stability analysis of the model

In this section, we analyse the stability of the model (2.1) at the DFE. First, we show the local stability of system (2.1) at the DFE.

Theorem 1. *The DFE of the model* (2.1) *is locally asymptotically stable if* $\mathscr{R}_0 < 1$*, and unstable if* $\mathscr{R}_0 > 1$.

Proof. Let $\bar{H} = (E_u(t), E_q(t), I_u(t), I_a(t), S_u(t), S_q(t), V_u(t), V_q(t), I_h(t), R(t))$, we can obtain the Jacobian matrix of the system corresponding to $\bar{H}$ at P_0, and partition the matrix.

It is given by

$$J(P_0) = \left(\begin{array}{cccc|cccccc} -K_1 + \eta_u M_1 & \theta\eta_u M_1 & M_1 & \eta_a M_1 & 0 & 0 & 0 & 0 & 0 & 0 \\ \alpha_u + \eta_u M_2 & -K_2 + \theta\eta_u M_2 & M_2 & \eta_a M_2 & 0 & 0 & 0 & 0 & 0 & 0 \\ f_1\sigma_u & 0 & -K_3 & 0 & 0 & 0 & 0 & 0 & 0 & 0 \\ (1 - f_1 - f_2)\sigma_u & (1 - r)\sigma_q & 0 & -K_5 & 0 & 0 & 0 & 0 & 0 & 0 \\ \hline * & * & * & * & -(\xi_v + d) & \omega & \eta_v & 0 & 0 & 0 \\ * & * & * & * & 0 & -(\omega + d) & 0 & 0 & 0 & 0 \\ * & * & * & * & \xi_v & 0 & -(\eta_v + d) & p_1\omega & 0 & 0 \\ * & * & * & * & 0 & 0 & 0 & -(p_1\omega + d) & 0 & 0 \\ * & * & * & * & 0 & 0 & 0 & 0 & -(\delta_h + \gamma_h + d) & 0 \\ * & * & * & * & 0 & 0 & 0 & 0 & \gamma_h & -d \end{array} \right)$$
$$= \begin{pmatrix} J_1 & J_2 \\ J_3 & J_4 \end{pmatrix}$$

Using the Laplace theorem, it's easy to find that the eigenvalues of $J(P_0)$ are determined by the eigenvalues of J_1 and J_4.

Consider the eigenvalues of J_4 first.

It is obvious that J_4 has always four negative eigenvalues $\lambda_1 = -d$, $\lambda_2 = -(\delta_h + \gamma_h + d)$, $\lambda_3 = -(p_1\omega + d)$ and $\lambda_4 = -(\omega + d)$, and the other eigenvalues of J_4 are determined by the equation

$$\lambda^2 + (\xi_v + \eta_v + 2d)\lambda + \xi_v d + \eta_v d + d^2 = 0.$$

Clearly, $\lambda_5 + \lambda_6 = -(\xi_v + \eta_v + 2d) < 0$, $\lambda_5 \cdot \lambda_6 = \xi_v d + \eta_v d + d^2 > 0$, so λ_5 and λ_6 are both negative.

Then consider the eigenvalues of J_1. Through calculation and integration, we have

$$\det(\lambda E - J_1) = a_0\lambda^4 + a_1\lambda^3 + a_2\lambda^2 + a_3\lambda + a_4 = 0,$$

where,

$$
\begin{aligned}
a_0 =&1,\\
a_1 =&K_1 + K_2 + K_3 + K_5 - \eta_u M_1 - \theta\eta_u M_2,\\
a_2 =&K_5(K_2 - \theta\eta_u M_2) - (1-r)\sigma_q\eta_a M_2 + (K_1 - \eta_u M_1)(K_2 + K_5 - \theta\eta_u M_2) + K_3(K_1 + K_2 + K_5 - \eta_u M_1\\
&- \theta\eta_u M_2) - \eta_a(1 - f_1 - f_2)\sigma_u M_1 + \theta\eta_u M_1(-\alpha_u - \eta_u M_2) - f_1\sigma_u M_1,\\
a_3 =&K_3[K_5(K_2 - \theta\eta_u M_2) - (1-r)\sigma_q\eta_a M_2 + (K_1 - \eta_u M_1)(K_2 + K_5 - \theta\eta_u M_2) - \eta_a(1 - f_1 - f_2)\sigma_u M_1\\
&+ \theta\eta_u M_1(-\alpha_u - \eta_u M_2)] + K_1[K_5(K_2 - \theta\eta_u M_2) - (1-r)\sigma_q\eta_a M_2] - \eta_u K_2 K_5 M_1 - \alpha_u\theta\eta_u K_5 M_1\\
&- \eta_a\alpha_u(1-r)\sigma_q M_1 - \eta_a(1 - f_1 - f_2)\sigma_u K_2 M_1 - f_1\sigma_u(K_2 + K_5)M_1,\\
a_4 =&K_3\{K_1[K_5(K_2 - \theta\eta_u M_2) - (1-r)\sigma_q\eta_a M_2] - \eta_u K_2 K_5 M_1 - \alpha_u\theta\eta_u K_5 M_1 - \eta_a\alpha_u(1-r)\sigma_q M_1\\
&- \eta_a(1 - f_1 - f_2)\sigma_u K_2 M_1 - f_1\sigma_u K_2 K_5 M_1\}.
\end{aligned}
$$

If $\mathscr{R}_0 < 1$, we have $\frac{\eta_u}{K_1}M_1 < 1$ and $\frac{\theta\eta_u}{K_2}M_2 < 1$, so it can be observed that $a_1 > 0$.

Because of $\frac{a_4}{K_1K_2K_3K_5} = 1 - \mathscr{R}_0$, we obtain $a_4 > 0$ if $\mathscr{R}_0 < 1$.

Due to

$$
\begin{aligned}
\frac{a_3}{K_1K_2K_3K_5} =& \frac{1}{K_1}[1 - \frac{\theta\eta_u}{K_2}M_2 - \eta_a\frac{(1-r)\sigma_q}{K_2K_5}M_2] + \frac{1}{K_5}(1 - \frac{\eta_u}{K_1}M_1 - \frac{\alpha_u\theta\eta_u}{K_1K_2}M_1 - \frac{\theta\eta_u}{K_2}M_2 - \frac{f_1\sigma_u}{K_1K_3}M_1)\\
&+ \frac{1}{K_2}[1 - \frac{\eta_u}{K_1}M_1 - \frac{f_1\sigma_u}{K_1K_3}M_1 - \eta_a\frac{(1 - f_1 - f_2)\sigma_u}{K_1K_5}M_1] + \frac{1}{K_3}\Big\{1 - \frac{\eta_u}{K_1}M_1 - \frac{\alpha_u\theta\eta_u}{K_1K_2}M_1\\
&- \frac{\theta\eta_u}{K_2}M_2 - \eta_a[\frac{(1 - f_1 - f_2)\sigma_u}{K_1K_5} + \frac{\alpha_u(1-r)\sigma_q}{K_1K_2K_5}]M_1 - \eta_a\frac{(1-r)\sigma_q}{K_2K_5}M_2\Big\}\\
>& \frac{1}{K_1}(1 - \mathscr{R}_{E_q} - \mathscr{R}_{I_a}) + \frac{1}{K_5}(1 - \mathscr{R}_{E_u} - \mathscr{R}_{E_q} - \mathscr{R}_{I_u}) + \frac{1}{K_2}(1 - \mathscr{R}_{E_u}\\
&- \mathscr{R}_{I_u} - \mathscr{R}_{I_a}) + \frac{1}{K_3}(1 - \mathscr{R}_{E_u} - \mathscr{R}_{E_q} - \mathscr{R}_{I_a})\\
>& 0,
\end{aligned}
$$

then $a_3 > 0$.

Meanwhile, we can also obtain that

$$
\begin{aligned}
a_1a_2 - a_3 =& (K_1 + K_2 + K_5 - \eta_u M_1 - \theta\eta_u M_2)[K_5(K_2 - \theta\eta_u M_2) - (1-r)\sigma_q\eta_a M_2 + K_1K_5 - \eta_u K_5 M_1\\
&- \eta_a(1 - f_1 - f_2)\sigma_u M_1] + (K_1 + K_2 + K_3 + K_5 - \eta_u M_1 - \theta\eta_u M_2)[K_3(K_1 + K_2 + K_5\\
&- \eta_u M_1 - \theta\eta_u M_2) - f_1\sigma_u M_1] + (K_1 + K_2 + K_5 - \eta_u M_1 - \theta\eta_u M_2)[K_1(K_2 - \theta\eta_u M_2)\\
&- \eta_u K_2 M_1 - \alpha_u\theta\eta_u M_1] - K_1K_5(K_2 - \theta\eta_u M_2) + \eta_u K_2 K_5 M_1 + \alpha_u\theta\eta_u K_5 M_1\\
&+ (1-r)\sigma_q\eta_a M_2 - \eta_a\alpha_u(1-r)\sigma_q M_1 - \eta_a(1 - f_1 - f_2)\sigma_u K_2 M_1\\
&+ f_1\sigma_u(K_2 + K_5)M_1\\
>& (K_1 + K_2 + K_5 - \eta_u M_1 - \theta\eta_u M_2)[K_5(K_2 - \theta\eta_u M_2) - (1-r)\sigma_q\eta_a M_2 + K_1K_5 - \eta_u K_5 M_1\\
&- \eta_a(1 - f_1 - f_2)\sigma_u M_1] + (K_1 + K_2 + K_3 + K_5 - \eta_u M_1 - \theta\eta_u M_2)K_3(K_2 + K_5 - \theta\eta_u M_2)\\
&+ (K_1 + K_2 - \eta_u M_1 - \theta\eta_u M_2)[K_1(K_2 - \theta\eta_u M_2) - \eta_u K_2 M_1 - \alpha_u\theta\eta_u M_1]
\end{aligned}
$$

$$
\begin{aligned}
&+ K_5K_1(K_2 - \theta\eta_u M_2) - K_5\eta_u K_2 M_1 - K_5\alpha_u\theta\eta_u M_1 - K_1K_5(K_2 - \theta\eta_u M_2)\\
&+ \eta_u K_2K_5M_1 + \alpha_u\theta\eta_u K_5M_1\\
&= (K_1 + K_2 + K_5 - \eta_u M_1 - \theta\eta_u M_2)[K_5(K_2 - \theta\eta_u M_2) - (1-r)\sigma_q\eta_a M_2 + K_1K_5 - \eta_u K_5M_1\\
&- \eta_a(1 - f_1 - f_2)\sigma_u M_1] + (K_1 + K_2 + K_3 + K_5 - \eta_u M_1 - \theta\eta_u M_2)K_3(K_2 + K_5 - \theta\eta_u M_2)\\
&+ (K_1 + K_2 - \eta_u M_1 - \theta\eta_u M_2)[K_1(K_2 - \theta\eta_u M_2) - \eta_u K_2M_1 - \alpha_u\theta\eta_u M_1]\\
&> 0.
\end{aligned}
$$

The first inequality is established due to $\left(\frac{\eta_u}{K_1} + \frac{f_1\sigma_u}{K_1K_3}\right)M_1 < 1$, if $\mathscr{R}_0 < 1$. It is apparent from the above analysis that it satisfies the Routh-Hurwitz stability criterion. Thus, it follows that the DFE P_0 is locally asymptotically stable if $\mathscr{R}_0 < 1$. On the other hand, we have $\frac{a_4}{K_1K_2K_3K_5} = 1 - \mathscr{R}_0 < 0$ if $\mathscr{R}_0 > 1$, then $a_4 < 0$, which shows that at least one of the eigenvalues of J_1 is positive. Therefore, the DFE P_0 is unstable if $\mathscr{R}_0 > 1$. This completes the proof. □

Theorem 2. *The DFE of the model* (2.1) *is globally asymptotically stable in* Ω *if* $\mathscr{R}_0 < 1$.

Proof. Let $\boldsymbol{X} = (E_u, E_q, I_u, I_h, I_a)^T$. It can be stated that

$$\frac{\mathrm{d}\boldsymbol{X}}{\mathrm{d}t} \leq (F - V)\boldsymbol{X},$$

with F and V are matrices on calculating $\mathscr{R}_0$. Let $\boldsymbol{u} = (\eta_u, \theta\eta_u, 1, 0, \eta_a)$. It then follows from the fact $\mathscr{R}_0 = \rho(FV^{-1}) = \rho(V^{-1}F)$ and direct calculation that $\boldsymbol{u}$ is a left eigenvector of the matrix $V^{-1}F$, i.e., $\boldsymbol{u}V^{-1}F = \mathscr{R}_0\boldsymbol{u}$.

Consider a Liapunov function

$$\mathscr{L}_0 = \boldsymbol{u}V^{-1}\boldsymbol{X}.$$

Differentiating the above equation, we have

$$\frac{\mathrm{d}\mathscr{L}_0}{\mathrm{d}t} = \boldsymbol{u}V^{-1}\frac{\mathrm{d}\boldsymbol{X}}{\mathrm{d}t} \leq \boldsymbol{u}V^{-1}(F - V)\boldsymbol{X} = \boldsymbol{u}(\mathscr{R}_0 - 1)\boldsymbol{X}.$$

If $\mathscr{R}_0 < 1$, the equality $\frac{d\mathscr{L}_0}{dt} = 0$ implies that $\boldsymbol{u}\boldsymbol{X} = 0$. This leads to $E_u = E_q = I_u = I_a = 0$ by noting that all components of $\boldsymbol{u}$ except for the fourth element are positive.

Clearly, let

$$E = \left\{\left(S_u, S_q, V_u, V_q, E_u, E_q, I_u, I_h, I_a, R\right) \in \Omega \mid \frac{d\mathscr{L}_0}{dt} = 0\right\} = \left\{E_u = E_q = I_u = I_a = 0\right\},$$

then the largest invariant set of the system in E is $M = \left\{E_u = E_q = I_u = I_a = 0\right\}$. By LaSalle's Invariant Principle [24], we get $\lim\limits_{t\to\infty} E_u(t) = \lim\limits_{t\to\infty} E_q(t) = \lim\limits_{t\to\infty} I_u(t) = \lim\limits_{t\to\infty} I_a(t) = 0$. Then, it is easy to solve the 8th equation of the model (2.1), and we have

$$I_h(t) = \left[I_{h0} + \int_0^t \left(f_2\sigma_u E_u(\tau) + r\sigma_q E_q(\tau) + \phi_u I_u(\tau) + \sigma_a I_a(\tau)\right)e^{K_4\tau}d\tau\right]e^{-K_4t}.$$

Using L'Hospital's rule,

$$\lim_{t\to\infty} I_h(t) = \lim_{t\to\infty} \frac{f_2\sigma_u E_u(t) + r\sigma_q E_q(t) + \phi_u I_u(t) + \sigma_a I_a(t)}{K_4} = 0.$$

In a similar way, for the 2nd, 4th and 10th equation of the model (2.1), we have $\lim_{t\to\infty} S_q(t) = \lim_{t\to\infty} V_q(t) = \lim_{t\to\infty} R(t) = 0$. Hence, we can obtain the limit system of (2.1) as follows.

$$\begin{aligned} \frac{\mathrm{d}S_u}{\mathrm{d}t} &= \Lambda - (\xi_v + d) S_u + \eta_v V_u, \\ \frac{\mathrm{d}V_u}{\mathrm{d}t} &= \xi_v S_u - (\eta_v + d) V_u. \end{aligned} \tag{3.2}$$

It is easy to solve that

$$\begin{aligned} S_u(t) &= S_0 + \left(S_u(0) - \frac{\Lambda(\eta_v + d)}{d(\eta_v + d + \xi_v)}\right) e^{-(\eta_v + d + \xi_v)t}, \\ V_u(t) &= V_0 + \left(V_u(0) - \frac{\Lambda\xi_v}{d(\eta_v + d + \xi_v)}\right) e^{-(\eta_v + d + \xi_v)t}. \end{aligned}$$

Clearly, we can get $\lim_{t\to\infty} S_u(t) = S_0$, $\lim_{t\to\infty} V_u(t) = V_0$, so (S_0, V_0) is globally attractive for the limit system (3.2). By discussion of linearization systems for (3.2), it can be known that (S_0, V_0) is locally asymptotically stable if $\mathscr{R}_0 < 1$. Combining global attraction of (S_0, V_0), we can obtain that (S_0, V_0) is globally asymptotically stable for the limit systems (3.2). It follows that $P_0(S_0, 0, V_0, 0, 0, 0, 0, 0, 0, 0)$ is globally attractive for the original system (2.1). In addition, combining Theorem 1, we eventually concluded that P_0 is globally asymptotically stable if $\mathscr{R}_0 < 1$. □

4. Numerical simulation of the system (2.1)

In this section, we present the numerical solution of the system (2.1).

We can get $\mathscr{R}_0 = 0.0147 < 1$ and $P_0 = (48.7179, 0, 51.2821, 0, 0, 0, 0, 0, 0, 0, 0, 0)$ by using the parameter values given in Table 2. The dynamical behavior for different initial conditions of model (2.1) is presented in Figure 2. It's easy to find that, S_u tends to 48.7179, S_q tends to 0, V_u tends to 51.2821, V_q tends to 0, E_u tends to 0, E_q tends to 0, I_u tends to 0, I_h tends to 0, I_a tends to 0, and R tends to 0. It shows that system (2.1) has a DFE and it is globally asymptotically stable with different initial values when $\mathscr{R}_0 < 1$. The numerical simulation results support the case stated in Theorem 2.

5. Empirical analysis

5.1. Data sources and methods

In order to show that the model is practical, the COVID-19 pandemic mainly caused by Delta variant in South Korea is analysed and verified in this section. The experimental data come from the Central Disaster Management Headquarters of Korea [25]. About 97% of confirmed cases were infected by the Delta variant on August 22, 2021 [26], so August 22, 2021 is chosen as the starting date of the data

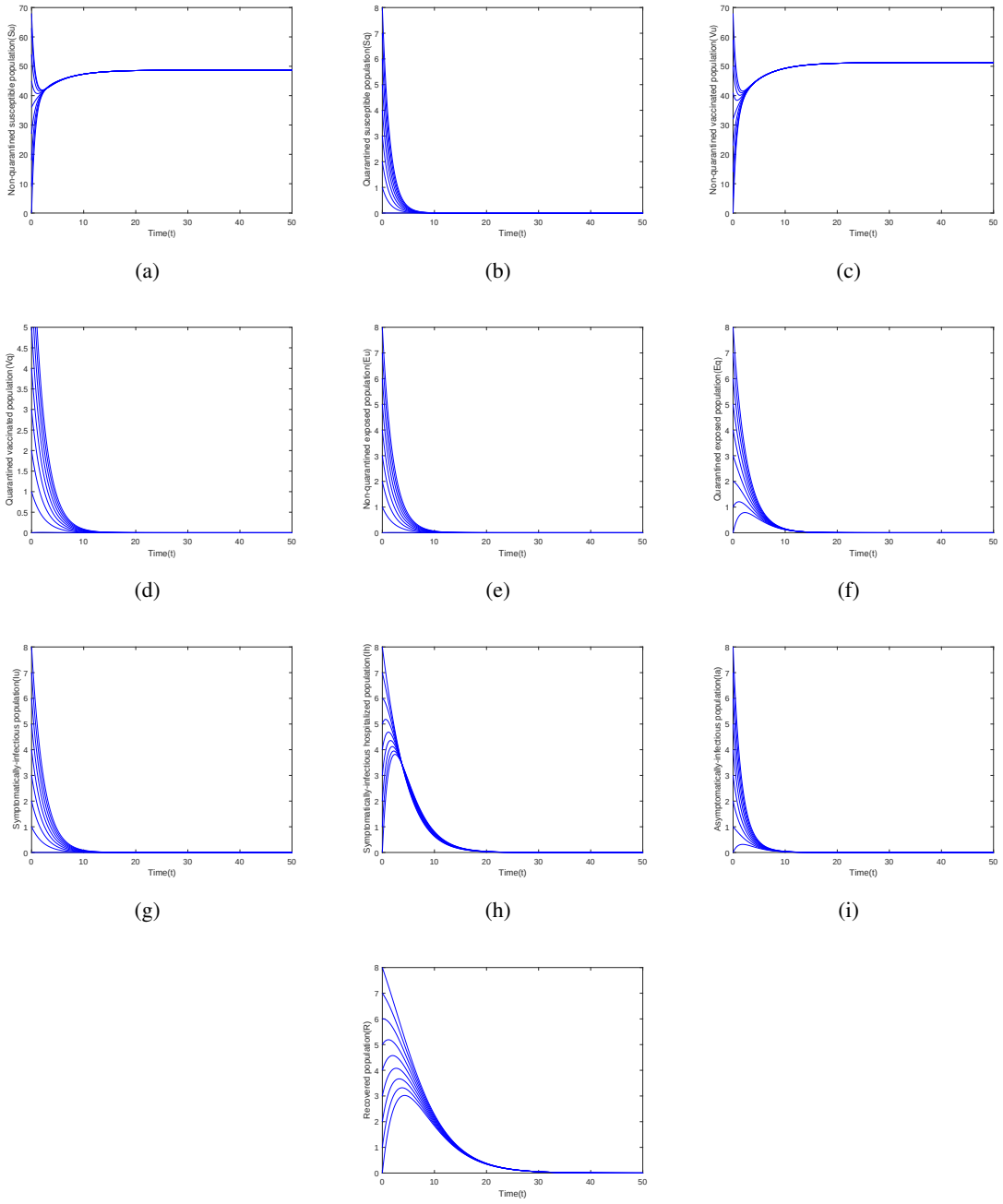

Figure 2. The dynamical behavior for different initial conditions of non-quarantined susceptible individuals S_u, quarantined susceptible individuals S_q, non-quarantined vaccinated individuals V_u, quarantined vaccinated individuals V_q, non-quarantined exposed individuals E_u, quarantined exposed individuals E_q, non-hospitalized symptomatically-infectious individuals I_u, hospitalized infectious individuals I_h, asymptomatically-infectious individuals I_a and recovered individuals R, subfigures (a)–(j) represent them, respectively.

set. The data in this paper is the official data of COVID-19 in Korea from August 22, 2021 to October 20, 2021.

In order to verify the training effect, the data set is divided into training set (from August 22 to October 14, 2021, 54 days in total) and verification set (from October 15 to 20, 2021, 6 days in total) according to the ratio of 9:1. The unknown parameters of the model are obtained by fitting the real data of the training set, and the prediction effect of the model is tested by using the real data of the verification set. According to the Korea Disease Control and Prevention Agency (KDCA) [27], since September 24, 2021, the vaccinated individuals can be exempted from quarantine if they show no symptoms after close contact with the confirmed individuals. Therefore, this paper considers the training set in two stages. The first stage is from August 22, 2021 to September 23, 2021, and the second stage is from September 24, 2021 to October 14, 2021.

5.2. Parameter fitting

Before fitting the parameters, we fix some parameters from previous literatures and studies to reduce the complexity.

Since the recommended duration in quarantine for people suspected of being exposed to COVID-19 in South Korea was 14 days [28], we set $\omega = 1/14$ per day. Further, Zhang et al. estimated that the mean incubation period of Delta variant was 4.4 days [29], which was shorter than that of the original strain reported by Yin et al. (4.4 vs. 6.8) [30]. Thus, we consider $\sigma_u = \sigma_q = 1/4.4$ per day. Some studies have suggested that most COVID-19 infections (over 95.6%) show moderate, mild, or asymptomatic infections, about 3.08% show severe symptoms (but without requiring ICU admission), and 1.32% show critically-severe symptoms requiring ICU admission [31, 32]. Consequently, we set $f_2 = 0.044$. According to [33], the proportion of asymptomatically-infectious individuals is 16%. Hence, we get f_1=0.80304 and $1 - f_1 - f_2$=0.15296 respectively. The modification parameter for the relative infectiousness of asymptomatically-infectious individuals (η_a) was estimated from [31, 34] to be 0.5, so we set $\eta_a = 0.5$. Due to the strict quarantine policy in South Korea [28], we assume that the ineffectiveness of quarantine $\theta = 0$. The average lifespan of Korean is 83.3 years [35]. Therefore, we have the natural death rate $d = 1/(83.3 \times 365)$ per day. The latest total population of South Korea is about $N(0)$=51,821,669 [36], hence, the recruitment rate Λ is obtained from $\Lambda/d = N(0)$, so $\Lambda = 1704.41$ per day. The World Health Organization (WHO) explicitly wrote in the document [37] that the critical characteristic or the minimal requirement is to confer protection for at least six months. Therefore, we assume that the average duration of vaccine immunity is 180 days, then $\eta_v = 1/180$ per day. It can be seen from [38] that COVID-19 vaccine was on average 86.6% effective in preventing infections, so we select ε_v =0.134. According to [39], the maximum and minimum values of disease-induced mortality rate from August 22 to October 14 were 0.93% and 0.82%, respectively, and we take the average value as 0.875%. Thus we set $\delta_u = \delta_h = 0.00875$ per day. To obtain estimation for δ_a, we assume that $\delta_a = 0.5\delta_u$ (so that $\delta_a = 0.004375$ per day). According to [39] and calculation, vaccination rate ξ_v is about 7.6×10^{-3} per day. As can be seen from [27], the vaccinated individuals, like the unvaccinated individuals, needed to be quarantined, so $p_1 = p_2 = 1$ in the first stage. However, since the vaccinated individuals did not need to be quarantined since September 24 [27], $p_1 = p_2 = 0$ in the second stage. In addition, we fix the initial hospitalized population $I_h(0)$ and total population $N(0)$ as 27,959 and 51,821,669 respectively according to the data information. From [40], it can be known the number of newly confirmed cases per day confirmed by temporary screening. Let the vaccination

proportion on August 22 be ξ. According to [41], ξ=22.5%. The default parameter values and the initial values of state variables are given in Tables 3 and 4, respectively.

Table 3. Parameter values from the literatures (and those assumed).

Parameter	Default values	Reference	Parameter	Default values	Reference
Λ	1704.41	[35, 36]	$1-f_1-f_2$	0.15296	[31, 32, 33]
d	$1/(83.3\times 365)$	[35]	r	0.7	[10]
ξ_v	7.6×10^{-3}	[39]	σ_a	0.2435	[10]
η_v	1/180	[37]	ϕ_u	1/5	[10, 31]
ε_v	0.134	[38]	p_1	1 0	[27]
η_u	0.5	Assumed	p_2	1 0	[27]
η_a	0.5	[31, 34]	γ_u	1/10	[10, 31]
θ	0	[28]	γ_h	1/8	[10, 31]
ω	1/14	[28]	γ_a	0.13978	[42]
$\sigma_u\left(\sigma_q\right)$	1/4.4	[29]	δ_u	0.00875	[39]
f_1	0.80304	[31, 32, 33]	δ_h	0.00875	[39]
f_2	0.044	[31, 32]	δ_a	0.004375	[39]

The remaining parameters are obtained by fitting the data in the training set. The model is solved by using lsqcurvefit function in Matlab, which utilizes a nonlinear least squares method to estimate parameters. The fitting parameters in two stages are given in Table 5.

5.3. Model fitting and prediction

In order to evaluate the fitting and prediction effect, the mean absolute percentage error (MAPE) is used in this paper. MAPE between the cumulative number of confirmed cases obtained by model fitting and the actual data in the training set is used to evaluate the fitting effect of the model. Similarly, MAPE between the cumulative number of confirmed cases obtained by model prediction and actual data in the verification set is used to evaluate the prediction effect of the model. MAPE is expressed as:

$$MAPE = \frac{1}{n}\sum_{t=1}^{n}\left|\frac{\hat{C}_t - C_t}{C_t}\right| \times 100\% \tag{5.1}$$

where, C_t is the actual cumulative number of confirmed cases on the t th day.

The best fits to the reported data of the two stages via our model are depicted in Figure 3. Further, using the above parameters, we make a prediction on the verification set, and the prediction result is shown in Figure 4. As can be seen, there is a good agreement between the prediction result and the real data. The fitting and prediction effect of the model are shown in Table 6.

6. Numerical simulations of quarantine and vaccine impact

For simplicity of presentation, we make $\theta_1 = 1-\theta$ and $\varepsilon = 1-\varepsilon_v$, i.e., θ_1 is quarantine effectiveness and ε is vaccine efficacy.

Table 4. Initial value of state variables.

Variable	Initial value	Reference
S_u	39,465,104	$(1-\xi)(N(0)-S_q(0)-V_q(0)-E_u(0)-E_q(0)-I_h(0)-I_u(0)-I_a(0)-R(0))$
S_q	478,691	Derived from the number of newly confirmed cases per day confirmed by temporary screening, ω and ξ
V_u	11,457,611	$\xi(N(0)-S_q(0)-V_q(0)-E_u(0)-E_q(0)-I_h(0)-I_u(0)-I_a(0)-R(0))$
V_q	138,975	Derived from the number of newly confirmed cases per day confirmed by temporary screening, ω and ξ
E_u	1664	Derived from $I_u(0)$, $I_a(0)$ and σ_u
E_q	4852	Derived from the number of newly confirmed cases per day confirmed by temporary screening and σ_q
I_u	1751	Derived from the proportion of symptomatically-infectious individuals, $I_h(0)$ and ϕ_u
I_h	27,959	Official data
I_a	333	Derived from the proportion of asymptomatically-infectious individuals, $I_h(0)$ and σ_a
R	244,729	Derived from official data and the proportion of newly confirmed cases per day confirmed by temporary screening

Table 5. Fitted parameters.

Parameter	Fitted value of the first stage	Fitted value of the second stage
c	10.7392	24.6129
β	0.1037	0.1216
q	0.7727	1
α_u	0.0714	0.3156

Table 6. Evaluation of fitting and prediction effect.

	Fitting effect of the first stage	Fitting effect of the second stage	Prediction effect
MAPE	0.23%	0.22%	0.047%

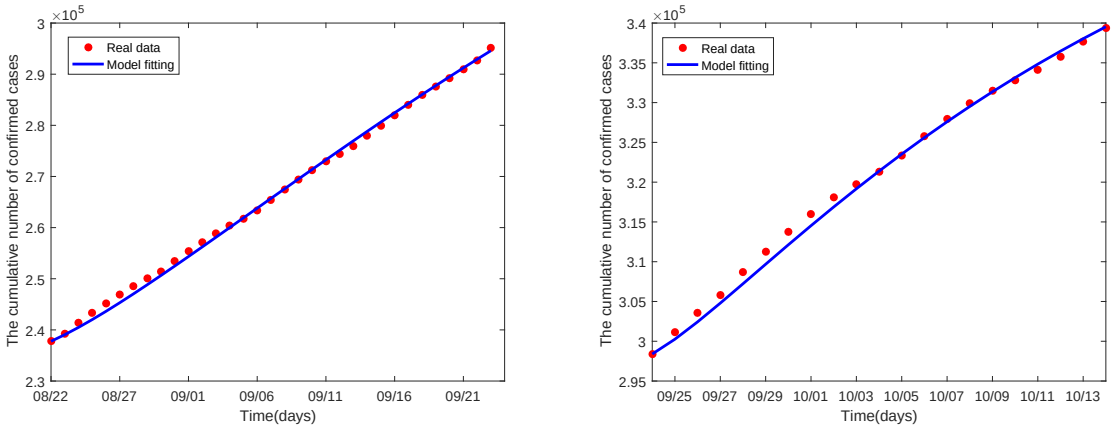

(a) (b)

Figure 3. Data fitting of the model (2.1) in the first and second stages using COVID-19 cumulative number of confirmed cases in South Korea, subfigures (a) and (b) represent them, respectively.

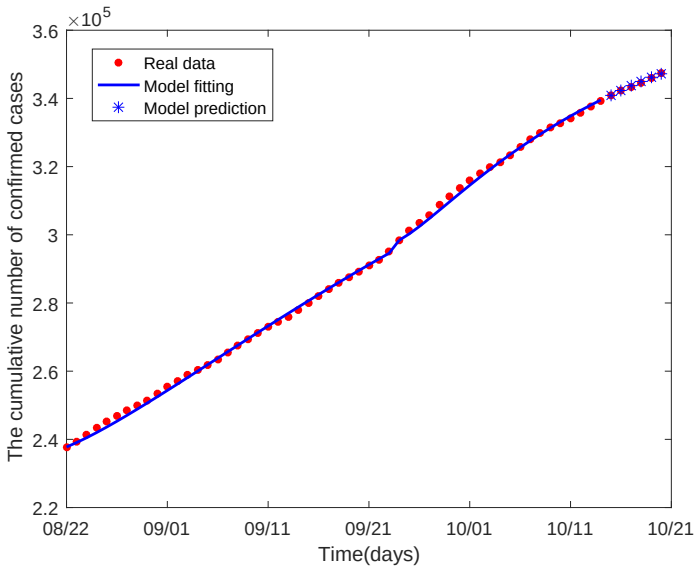

Figure 4. Prediction of the model (2.1) (using the estimated parameters).

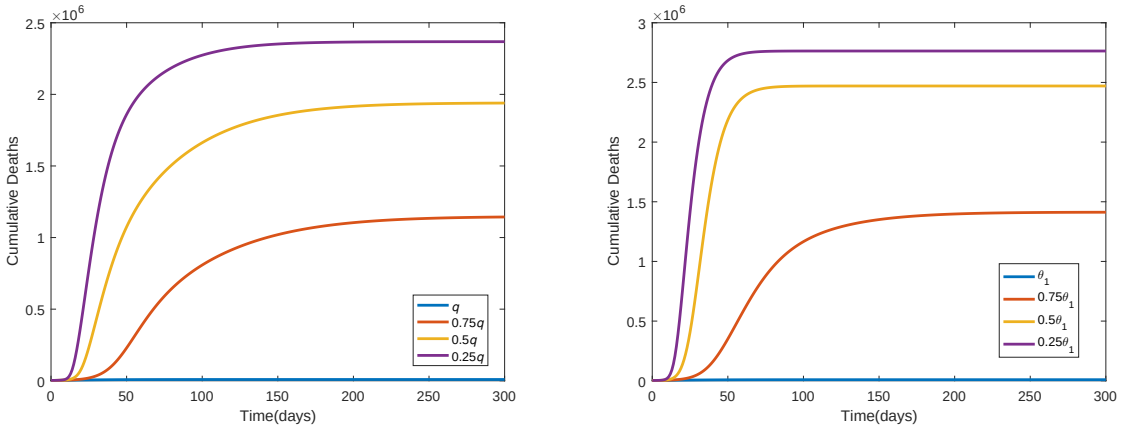

(a) (b)

Figure 5. The cumulative number of deaths for various values of q and θ_1, subfigures (a) and (b) represent them, respectively.

6.1. Numerical simulations of quarantine impact

First of all, we simulate the impact of the quarantine rate (q) on the spread of COVID-19. As shown in the Figure 5(a), if the quarantine rate decreases, the cumulative number of deaths will sharply increase, which negatively affects prevention and control of COVID-19.

Next, we consider the impact of quarantine effectiveness (θ_1) on COVID-19 transmission. The results are shown in Figure 5(b), which imply that implementing strict quarantine measures is an effective means to prevent the development of the COVID-19 pandemic.

6.2. Numerical simulations of vaccine impact

We firstly assess the impact of the vaccination rate (ξ_v) on the prevention of COVID-19 transmission. The simulation results are presented in Figure 6(a), which show that a significantly large increasement in vaccination rate is necessarily needed for the control of COVID-19.

As can be seen from the comparison results in Figure 6(b), when we increase vaccine efficacy (ε), the cumulative number of deaths markedly decreases. Meanwhile, it is easy to find that the stronger the effectiveness of vaccine, the faster the elimination of pandemic.

Finally, we simulate the impact of rate of immunity loss (η_v) on dynamic transmission of the COVID-19. Depicted in Figure 6(c), the longer duration of vaccine immunity can have a better suppression effect on the spread of pandemic.

7. Discussion

A mathematical model for mutated COVID-19 combining quarantine, isolation and vaccination is established in this paper, and it is proved that the model is globally asymptotically stable at the DFE if $\mathscr{R}_0 < 1$, and the correctness of this result is verified by numerical simulation. The unknown parameters are obtained by fitting the COVID-19 epidemic data in South Korea from August 22 to October 14, 2021 in stages, and MAPE in two stages are 0.23 and 0.22%, respectively. The fitting effect of the

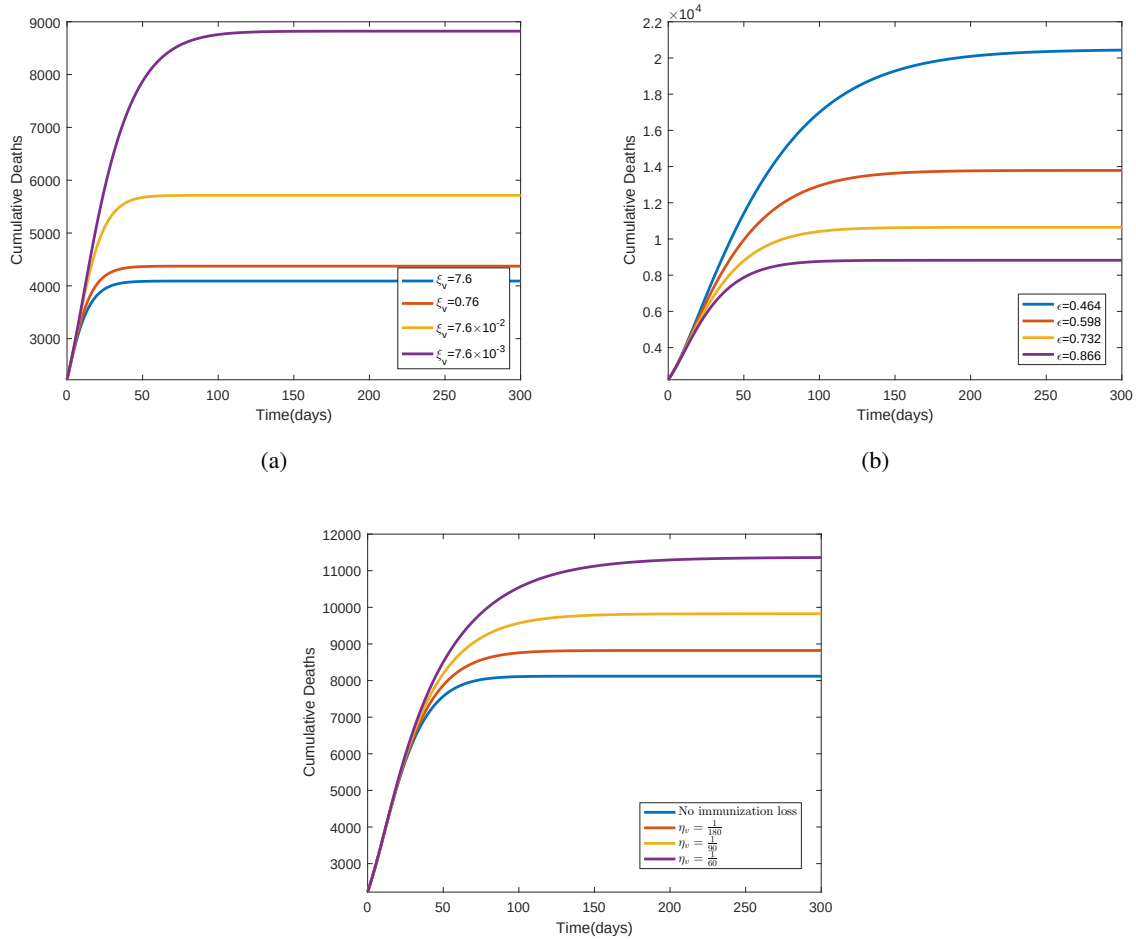

Figure 6. The cumulative number of deaths for various values of ξ_v, ε and η_v, subfigures (a), (b) and (c) represent them, respectively.

model is satisfying. In the prediction of the data set from October 15 to October 20, 2021, MAPE is 0.047%, and the prediction effect is satisfactory, which also shows that the model is feasible. Numerical simulations indicate that it is essential to implement strict quarantine measures and strengthen contact tracing for combating the spread of COVID-19. Meanwhile, increasing vaccination rate and getting the vaccines with more effective and the longer duration of vaccine immunity have positive impact on the prevention of pandemic transmission.

However, there are still many issues worthy of further study. For instance, most parameters (such as quarantine rate and vaccination rate) are dynamically changing during the development of COVID-19, but these characteristics are not taken into account in the current model. Thus, dynamic model with stochastic parameters deserves further study. Besides, the severity of infection is different in reality, so we can consider further the confirmed individuals with common and severe symptoms. These problems are of great interest which can be left for studying in the near further.

Acknowledgements

The authors are grateful to the editors and the reviewers for their valuable comments and suggestions. This work was supported by the Fundamental Research Funds for the Central Universities (NO.2572018BC20).

Conflict of interest

The authors declare there is no conflict of interest.

References

1. Q. Li, X. H. Guan, P. Wu, X. Y. Wang, L. Zhou, Y. Q. Tong, et al., Early transmission dynamics in Wuhan, China, of novel coronavirus–infected pneumonia, *N. Engl. J. Med.*, **382** (2020), 1199–1207. https://doi.org/10.1056/NEJMoa2001316
2. *World Health Organization*, WHO coronavirus disease (COVID-19) dashboard, 2022. Available from: https://covid19.who.int/.
3. C. C. John, V. Ponnusamy, S. K. Chandrasekaran, R. Nandakumar, A survey on mathematical, machine learning and deep learning models for COVID-19 transmission and diagnosis, *IEEE Rev. Biomed. Eng.*, **15** (2021), 325–340. https://doi.org/10.1109/RBME.2021.3069213
4. Z. H. Yu, A. Sohail, T. A. Nofal, J. M. R. S. Tavares, Explainability of neural network clustering in interpreting the COVID-19 emergency data, *Fractals*, (2021). https://doi.org/10.1142/S0218348X22401223
5. Z. H. Yu, A. S. G. Abdel-Salam, A. Sohail, F. Alam, Forecasting the impact of environmental stresses on the frequent waves of COVID19, *Nonlinear Dyn.*, **106** (2021), 1509–1523. https://doi.org/10.1007/s11071-021-06777-6
6. Z. H. Yu, R. Ellahi, A. Nutini, A. Sohail, S. M. Sait, Modeling and simulations of CoViD-19 molecular mechanism induced by cytokines storm during SARS-CoV2 infection, *J. Mol. Liq.*, **327** (2021), 114863. https://doi.org/10.1016/j.molliq.2020.114863
7. Z. H. Yu, H. X. Gao, D. Wang, A. A. Alnuaim, M. Firdausi, A. M. Mostafa, SEI^{2}RS malware propagation model considering two infection rates in cyber-physical systems, *Physica A*, **597** (2022), 127207. https://doi.org/10.1016/j.physa.2022.127207
8. Z. H. Yu, S. Lu, D. Wang, Z. W. Li, Modeling and analysis of rumor propagation in social networks, *Inf. Sci.*, **580** (2021), 857–873. https://doi.org/10.1016/j.ins.2021.09.012
9. N. Perra, Non-pharmaceutical interventions during the COVID-19 pandemic: A review, *Phys. Rep.*, **913** (2021), 1–52. https://doi.org/10.1016/j.physrep.2021.02.001
10. C. N. Ngonghala, E. Iboi, S. Eikenberry, M. Scotch, C. R. MacIntyre, M. H. Bonds, et al., Mathematical assessment of the impact of non-pharmaceutical interventions on curtailing the 2019 novel Coronavirus, *Math. Biosci.*, **325** (2020), 108364. https://doi.org/10.1016/j.mbs.2020.108364
11. Z. H. Yu, R. Arif, M. A. Fahmy, A. Sohail, Self organizing maps for the parametric analysis of COVID-19 SEIRS delayed model, *Chaos Solitons Fractals*, **150** (2021), 111202. https://doi.org/10.1016/j.chaos.2021.111202

12. M. Jeyanathan, S. Afkhami, F. Smaill, M. S. Miller, B. D. Lichty, Z. Xing, Immunological considerations for COVID-19 vaccine strategies, *Nat. Rev. Immunol.*, **20** (2020), 615–632. https://doi.org/10.1038/s41577-020-00434-6

13. T. J. Bollyky, US COVID-19 vaccination challenges go beyond supply, *Ann. Intern. Med.*, **174** (2021), 558–559. https://doi.org/10.7326/M20-8280

14. E. A. Iboi, C. N. Ngonghala, A. B. Gumel, Will an imperfect vaccine curtail the COVID-19 pandemic in the US?, *Infect. Dis. Model.*, **5** (2020), 510–524. https://doi.org/10.1016/j.idm.2020.07.006

15. B. Huang, J. H. Wang, J. X. Cai, S. Q. Yao, P. K. S. Chan, T. H. Tam, et al., Integrated vaccination and physical distancing interventions to prevent future COVID-19 waves in Chinese cities, *Nat. Hum. Behav.*, **5** (2021), 695–705. https://doi.org/10.1038/s41562-021-01063-2

16. Y. K. Zou, W. Yang, J. J. Lai, J. W. Hou, W. Lin, Vaccination and quarantine effect on COVID-19 transmission dynamics incorporating Chinese-Spring-Festival travel rush: Modeling and simulations, *Bull. Math. Biol.*, **84** (2022), 1–19. https://doi.org/10.1007/s11538-021-00958-5

17. *World Health Organization*, Coronavirus disease (COVID-19): Variants of SARS-COV-2, 2022. Available from: https://www.who.int/emergencies/diseases/novel-coronavirus-2019/question-and-answers-hub/q-a-detail/coronavirus-disease-(covid-19)-variants-of-sars-cov-2.

18. *World Health Organization*, Coronavirus disease (COVID-19): Vaccines, 2022. Available from: https://www.who.int/emergencies/diseases/novel-coronavirus-2019/question-and-answers-hub/q-a-detail/coronavirus-disease-(covid-19)-vaccines.

19. T. T. Li, Y. M. Guo, Modeling and optimal control of mutated COVID-19 (Delta strain) with imperfect vaccination, *Chaos Solitons Fractals*, **156** (2022), 111825. https://doi.org/10.1016/j.chaos.2022.111825

20. A. Truszkowska, L. Zino, S. Butail, E. Caroppo, Z. P. Jiang, A. Rizzo, et al., Predicting the effects of waning vaccine immunity against COVID-19 through high-resolution agent-based modeling, *Adv. Theory Simul.*, (2022), 2100521. https://doi.org/10.1002/adts.202100521

21. V. Lakshmikantham, S. Leela, A. A. Martynyuk, *Stability analysis of nonlinear systems*, Marcel Dekker, Inc., New York and Basel, 1989. https://doi.org/10.1007/978-3-319-27200-9

22. P. Van den Driessche, J. Watmough, Reproduction numbers and sub-threshold endemic equilibria for compartmental models of disease transmission, *Math. Biosci.*, **180** (2002), 29–48. https://doi.org/10.1016/S0025-5564(02)00108-6

23. O. Diekmann, J. A. P. Heesterbeek, J. A. J. Metz, O. Diekmann, On the definition and the computation of the basic reproduction ratio R_0 in models for infectious diseases in heterogeneous populations, *J. Math. Biol.*, **28** (1990), 365–382.

24. J. P. LaSalle, *The stability of dynamical systems*, Regional Conf. Ser. Appl. Math., SIAM, Philadelphia, 1976.

25. *Central Disaster Management Headquarters of Korea*, 2021. Available from: http://ncov.mohw.go.kr.

26. *Our World in Data*, 2021. Available from: https://ourworldindata.org/coronavirus#explore-the-global-situation.

27. *Korea Disease Control and Prevention Agency*, 2021. Available from: https://www.kdca.go.kr/index.es?sid=a2.

28. *Central Disaster Management Headquarters of Korea*, What is the criteria for releasing an asymptomatic person who tests positive for the virus from quarantine?, 2021. Available from: http://ncov.mohw.go.kr/en/faqBoardList.do?brdId=13&brdGubun=131&dataGubun=&ncvContSeq=&contSeq=&board_id=.

29. M. Zhang, J. P. Xiao, A. P. Deng, Y. T. Zhang, Y. L. Zhuang, T. Hu et al., Transmission dynamics of an outbreak of the COVID-19 Delta variant B. 1.617. 2–Guangdong Province, China, May–June 2021, *China CDC Wkly*, **3** (2021), 584–586. https://doi.org/10.46234/ccdcw2021.148

30. M. Z. Yin, Q. W. Zhu, X. Lü, Parameter estimation of the incubation period of COVID-19 based on the doubly interval-censored data model, *Nonlinear Dyn.*, **106** (2021), 1347–1358. https://doi.org/10.1007/s11071-021-06587-w

31. N. Ferguson, D. Laydon, G. Nedjati-Gilani, N. Imai, K. Ainslie, M. Baguelin, et al., Report 9: Impact of non-pharmaceutical interventions (NPIs) to reduce COVID19 mortality and healthcare demand, *Imperial College London*, **10** (2020), 491–497. https://doi.org/10.25561/77482

32. S. M. Kissler, C. Tedijanto, E. Goldstein, Y. H. Grad, M. Lipsitch, Projecting the transmission dynamics of SARS-CoV-2 through the postpandemic period, *Science*, **368** (2020), 860–868. https://doi.org/10.1126/science.abb5793

33. O. Byambasuren, M. Cardona, K. Bell, J. Clark, M. L. McLaws, P. Glasziou, Estimating the extent of asymptomatic COVID-19 and its potential for community transmission: systematic review and meta-analysis, *J. Assoc. Med. Microbiol. Infect. Dis. Can.*, **5** (2020), 223–234. https://doi.org/10.3138/jammi-2020-0030

34. R. Y. Li, S. Pei, B. Chen, Y. M. Song, T. Zhang, W. Yang, et al., Substantial undocumented infection facilitates the rapid dissemination of novel coronavirus (SARS-CoV-2), *Science*, **368** (2020), 489–493. https://doi.org/10.1126/science.abb3221

35. *SOUTH KOREA, Average Lifespan*, The information of average lifespan in South Korea, 2021. Available from: https://m.naver.com/.

36. *SOUTH KOREA, Population*, The information of population in South Korea, 2021. Available from: https://m.naver.com/.

37. *World Health Organization*, WHO target product profiles for COVID-19 vaccines, 2021. Available from: https://www.who.int/publications/m/item/who-target-product-profiles-for-covid-19-vaccines.

38. *Korea Disease Control and Prevention Agency*, Are COVID-19 vaccinations effective, 2021. Available from: https://ncv.kdca.go.kr/menu.es?mid=a20102000000.

39. *Central Disaster Management Headquarters of Korea*, 2021. Available from: http://ncov.mohw.go.kr/tcmBoardList.do?brdId=3&brdGubun=.

40. *Korea Disease Control and Prevention Agency*, 2021. Available from: http://www.kdca.go.kr/board/board.es?mid=a20501010000&bid=0015.

41. *Korea Disease Control and Prevention Agency*, The outbreak and vaccination status of COVID-19 in Korea (8.23., as of 0:00), 2021. Available from: https://www.kdca.go.kr/board/board.es?mid=a20501010000&bid=0015&list_no=716586&cg_code=&act=view&nPage=20.

42. B. Tang, X. Wang, Q. Li, N. L. Bragazzi, S. Y. Tang, Y. N. Xiao, et al., Estimation of the transmission risk of the 2019-nCoV and its implication for public health interventions, *J. Clin. Med.*, **9** (2020), 462. https://doi.org/10.3390/jcm9020462

AIMS Press